Int. J. Nanosci. Nanotechnol., Vol. 19, No. 3, Sept. 2023, pp. 135-147
DOI: 10.22034/ijnn.2023.560608.2262

Biosynthesis, Characterization of Nickel (II) Oxide Nanoparticles NiO and their High-Efficient Photocatalytic Application

Brahim El Ghmari*, Hanane Farah and Abdellah Ech-Chahad

Physical-Chemistry of Processes and Materials Laboratory, Department of Applied Chemistry and Environment, Faculty of Science and Technology, Hassan First University of Settat, 26000, Settat, Morocco

(*) Corresponding author: braxgh@gmail.com
(Received: 21 August 2022 and Accepted: 16 August 2023)

Abstract

This work sought to compare the photocatalytic efficiency of nickel (II) oxide nanoparticles (NiO-NPs) for the degradation of methylene blue (MB) and Rhodamine B dye (Rh B). NiO-NPs were synthesized by a green, simple and easy route using the plant extract H. Hirsuta. The morphological characteristics of the synthesized NiO NPs were characterized by SEM. In addition, UV-vis, XRD, FTIR and EDS analyses were also performed to investigate the optical properties, crystal size, functional groups and elemental composition of the NPs. These NiO NPs have a crystallinity size of 20.82 nm, and then were used for photocatalytic degradation of MB and Rh B in the presence of visible light irradiation. The photocatalytic degradation rate under optimal conditions of MB and Rh B was found to be 97.19% and 79.42% , respectively. The kinetic study of photocatalytic degradation followed pseudo-first-order kinetics for MB and Rh B dyes. In addition, NiO-NPs were used for a 4-nitrophenol reduction activity reaching 91.17% for 3 cycles.

Keywords: *Nickel oxide nanoparticles NiO-NPs, H. Hirsuta plant extract, 4-nitrophenol, Dye degradation, Methylene blue, Rhodamine B.*

1. INRODUCTION

At present, many environmental problems have arisen due to the impact of various natural and man-made factors on the earth's crust. In general, any unnecessary and unacceptable modification of the environment due to various human activities is called pollution. The direct or indirect alteration of biological, chemical, and physical properties of natural water flows has adverse effects not only on human life but also on aquatic ecosystems. There are different types of factors responsible for the pollution of natural water bodies, such as population explosion, urbanization, rapid industrialization, and water pollution, etc. Among all the factors of rapid industrialization, textile, food, dyeing, and paper industries are the primary sources of water pollution. The effluents from these industries contain various types of dyes and organic pollutants. Organic dye contamination is believed to play an active role in the pollution of aquatic ecosystems. Approximately 10-15% of the total global dye production is lost to wastewater during various processes [1]. Dyes in wastewater prevent sunlight from entering waterways, thereby reducing photosynthetic reactions. Some dyes are lethal, even neoplastic and malignant, and can pose a serious threat to human and animal health [2]. Contamination of industrial effluents with MB and Rh B dyes is a major problem and has a detrimental effect on both types of ecosystems. With the scarcity of water and awareness of the threats posed by industrial effluents, international environmental standards impose many stringent requirements worldwide, which has led to the development of innovative frameworks and techniques to remove dyes and other

organic pollutants from wastewater before discharge [3]. In recent years, in this rapidly evolving technological era, nanotechnology has received a tremendous boost, generating a multitude of scientific ideas that compete with the everyday challenges of growing technology [4]. Nanomaterials have attracted diverse scientific and technological interests due to their countless applications and specific properties [4]. These properties are conferred by their characteristic size, shape, and surface type. Among these nanostructures, TiO_2 is the most studied [5]. Recent studies on the photocatalytic activity of many p-type semiconducting transition metal oxides such as NiO, Cu_2O, FeO, etc. have appeared in the literature [6, 7].

In recent years, several studies have been conducted in the field of nanotechnology, using green plant materials and extracts for the biosynthesis of metal oxide nanoparticles to avoid chemicals responsible for environmental pollution [8]. The biosynthesis of metal nanoparticles follows a green process using different plant fractions as reducing and stabilizing agents. Among the many metal nanoparticles studied, nickel oxide is a valuable material used in various fields because of its unique properties [9]. Therefore, it is of great importance in the field of nanomaterials. Its properties are photoelectric, catalysis and drug delivery, and cathode in rechargeable batteries [10]. The increase in industrial activities always involves great pollution of the environment by chemicals, because due to the inadequacy of treatment systems, it is urgent to find simple and less expensive solutions, among which we find nanoparticles, which have already shown their potential application in the treatment of organic pollutants such as Methylene Blue and Rhodamine B, widely used in several areas: chemistry, pharmacology, medicine, biology, textile [11]. The unknowing use of this substance causes serious damage to human health and the environment [12]. Green synthesis is a modern field of biotechnology that represents an environmentally friendly and economical alternative to chemical and physical processes that are often harmful to the environment. Because in this method, natural reagents are biologically harmless, non-toxic, and environmentally friendly [9], Cymbopogon citratus [13], Petiveria alliacea L. [14], Paeonia emodi [15], Ziziphora clinopodioides [16], Callistemon lanceotus (Myrtaceae) [17, 18], Centella Asiatica and Tridax [19], and many others have been used in the biosynthesis of metal oxide nanoparticles [20].

In the green synthesis of metal oxide nanoparticles, researchers have used plant extracts widely available in nature. Due to its speed, environmental efficiency, and low cost, which are known as "vital plants". It has the power to absorb minerals while respecting safety levels [21]. These methods include algae, and microbes such as fungi, bacteria, and viruses as reducing agents [18, 22]. The current method has more than one advantage as it is an economical technique that is solvent and surfactant-free [23].

Studies on the use of nanostructured NiO as a photocatalyst for the degradation of organic dyes such as MB, Rh B, methyl orange, and acid red 1 have been reported [24, 25]. These reports indicate the potential applications of nanocrystalline NiO as a photocatalyst for many other reactions, including the degradation of organic pollutants for water purification, as well as the reduction activity of 4-nitrophenol [26, 27]. NiO-NPs are chemically stable and exhibit very high electro-optical performance with a wide band gap (3.6-4.0 eV). NiO is a p-type semiconductor widely used in many chemical and physical applications such as catalysis, solar cells, and gas sensing [28, 29]. According to the literature, there are several methods to prepare NiO-NPs, such as thermal decomposition [30], combustion [31], sol-gel [32, 33], co-precipitation [34],

spray pyrolysis [35], and the anodic arc plasma method [36].

The present study focuses on simple chemical synthesis, which has the advantage over other methods of being simple, fast, and energy-efficient [37]. Research around the world attempts to use industrial and natural precursors that are generally expensive. Despite this, H. Hirsuta extract was used in this study due to its accessibility and price. The product obtained presents the best photocatalytic activity towards MB and Rh-B dyes which are more used in different industrial fields. We report the synthesis and characterization of NiO monocrystalline with a high specific surface area by simple and direct green synthesis. The comparative study of the photocatalytic performance of NiO-NPs for the degradation of MB, and Rh-B dyes was carried out by adopting the different optimized parameters, namely: the influence of pH, irradiation time, and initial dye concentration. This is the first report of a comparative study on the photocatalytic performance of NiO-NPs biosynthesized by the plant extract of H. Hirsuta. In addition, the reduction property of 4-nitrophenol was investigated.

2. MATERIALS AND METHODS

2.1. Materials

The products used are: Nickel (II) nitrate $Ni(NO_3)_2,6H_2O$ (98%, MONTPLET& ESTEBAN SA BARCELONA.MADRID. Spain), the plant H. Hirsuta was harvested from the province of Ouezzane in the North of Morocco, sodium hydroxide (98%, LOBA CHEMIE PVT.LTD. India). The glassware used was washed with acetic acid and rinsed with distilled water. Two mortars, one made of porcelain and the other of zirconium, and a laboratory muffle furnace of 1200 ºC.

2.2. Preparation of H. Hirsuta Plant Extract

The plant H. Hirsuta was harvested during June, dried, and stored in the dark at room temperature. After about two months, the H. Hirsuta plant was washed twice with distilled water and dried at room temperature for 48 hours, then ground to a fine powder. 10 g of the H. Hirsuta was added to 400 ml in a 500 ml beaker. The mixture was shaken vigorously at 5 000 rpm and at room temperature overnight. The resulting extract was filtered through a piece of cloth and stored in a container. Finally, the filtrate was centrifuged at a speed of 10 000 rpm at room temperature to obtain a light brown supernatant and stored in a lightproof container for future use.

2.3. Biosynthesis of Nickel Oxide Nanoparticles (NiO-NPs)

NiO-NPs were synthesized by Co-precipitation method, using the plant extract H. Hirsuta. In a 250 ml beaker, 20 ml of nickel (II) nitrate solution Ni $(NO_3)_2$, $6H_2O$ (5 mM) was added to 60 ml of H. Hirsuta plant extract with extract:salt ratio (3:1) under stirring at 7000 rpm at room temperature for 10 min. The formation of the biosynthesized NiO-NPs was monitored by the color change and appearance of a green precipitate after a duration of 5 min and confirmed by UV-Vis spectroscopy after adjusting the pH = 8 with sodium hydroxide solution (0.1 M). Finally, the mixture was centrifuged at a speed of 10 000 rpm at room temperature to remove the supernatant, the precipitate was washed twice with distilled water and methanol, dried in an oven at a temperature of 70°C for 24 h, and calcined at 500°C in a muffle furnace before being placed in a glass container and stored for further analysis and applications.

2.4. Characterization of Nickel Oxide Nanoparticles (NiO-NPs) Biosynthesized

2.4.1. UV- vis Spectroscopy

The production of biosynthesized NiO-NPs was monitored using UV-visible spectra (DR 6.000 spectrophotometer with RFID technology (HACHLANGE, GERMANY)). Measurements were

performed under normal temperature and pressure conditions (20°C and 1atm) in the wavelength range 250-800 nm using a quartz cell.

2.4.2. X-ray Diffraction (XRD)

The crystal structure of the biosynthesized NiO-NPs was determined using an X-ray powder diffractometer (PhaserD2 diffractometer, Broker, USA) with Cu- Kα radiation of wavelength λ = 0.15406 nm in the range of 10°-80°, operated at 30 kV and 10 mA.

2.4.3. Fourier Transform Infrared Spectroscopy FTIR

Various functional groups were observed by FTIR spectral analysis (Varian 800 / Gladiatr model (Scimitar series, Australia / Pike Technologies, USA) such as carbonyls, polyphenols, and amides, which could be reductants for the biosynthesis of NiO-NPs.

2.4.4. Scanning Electron Microscopy (FESEM/EDS)

The morphology and shape of biosynthesized NiO-NPs were studied using scanning electron microscopy coupled to EDS (SEM-JEOL IT500HR) with the following properties: landing voltage 10.0 kV, WD 11.0 mm, quantification method ZAF, magnification x8500, vacuum mode high vacuum.

2.5. Catalytic Activity of Biosynthesized NiO-NPs

2.5.1 Catalytic Degradation of Methylene Blue and Rhodamine B Dyes

In a typical experiment, 1 mg of synthesized NiO-NPs was added to 50 ml (5 $mg.L^{-1}$) of an aqueous solution of MB and Rh B. Then, the solution was kept in earlen Mayer (reactor) with continuous stirring to ensure that the catalyst suspensions were uniform for the duration of the reaction. Meanwhile, after adjusting the pH (pH=10 for MB, and pH=2 for Rh B), an adequate amount of dye solution was removed and filtered to separate the NiO-NPs. Then, the filtrate solution was analyzed using a UV-Vis spectro-photometer at the maximum absorption wavelength 663 nm and 554 nm of the dye to obtain the concentration of MB and Rh-B in the solution. The percentage of dye degradation was calculated using Equation 1.

$$D(\%) = \frac{A_0 - A_t}{A_0} \times 100 \qquad (1)$$

In which A0 and At Stand as the absorbance ago of radiation and at time t, respectively.

2.6. Reduction of 4-Nitrophenol (4-NP) by NiO-NPs and reusability

The reduction experiments of 4-nitrophenol (4-NP) were performed as follows: An aqueous solution of 4-NP (60 ml, 5 10^{-5} M) was mixed with a freshly prepared $NaBH_4$ solution (1.5 10^{-4} M, 15 ml), resulting in a dark yellow solution. Then 5 mg of catalyst (prepared as above) was dispersed in the solution, followed by sonication for 1 min. After adjusting the pH =9, the progress of the reaction for all experiments was monitored using a UV-vis spectrophotometer [26]. The reuse of NiO-NPs was performed for 3 cycles, at the end of the first reduction experiment, the catalyst was collected by centrifugation, washed with water and ethanol, and then oven dried at 80°C for 3h for the next cycle.

3. RESULTS AND DISCUSSION

3.1. Characterization of Nickel Oxide Nanoparticles NiO-NPs

3.1.1. UV- vis Spectroscopy and Optical Bandgap

Preliminary studies suggest that phytochemical screening of H. Hirsuta plant extract detects the presence of polyphenols, flavonoids, and condensed tannins [38, 39]. The colloidal solution of $Ni(OH)_2$ was thus prepared and the plant extract was analyzed by UV-Vis spectroscopy (see Fig. 1(a-b)). Indeed, the spectrum of the plant extract showed two peaks at 300 nm and 670 nm. After the reaction, the spectrum of $Ni(OH)_2$ showed

that there is a peak at 390 nm. This peak corresponds to the characteristic absorption band of the surface plasmon resonance of the $Ni(OH)_2$ precipitate in solution [40]. Fig. 2 shows the UV-vis spectrometer of NiO-NPs obtained after calcination, the peak indicated at 301 nm is attributed to the NiO-NPs [41].

Determination of the Optical Bandgap

In general, the optical band gap of a semiconductor can be determined by plotting the absorption coefficient versus photon energy, which could be estimated using the Tauc's formula (equation (2)) [42]:

$$(\alpha h\nu) = K(h\nu - E_g)^n \quad (2)$$

where α is the absorption coefficient, hν is the incident photon energy, K is a constant, Eg is the optical band gap in electron volts (eV) and n is an exponent that can take two values depending on the nature of the electronic transition, i.e.; n = 2 for a direct transition, and n = 1/2 for an indirect transition as shown in fig. 3(a-b) [43, 44].

Estimation of the Urbach Energy

The Urbach energy is related to the width of the band tails of localized states. The Urbach energy is determined from equation (2) from the slope of the linear part of the plot of $\ln(\alpha)$ versus photon energy $h\nu$ (Fig. 4) [45] . The results are presented in table 1, and a report on the band gap energy values of NiO-NPs in table 2.

$$\ln(\alpha) = \frac{h\nu}{Eu} + ln(\alpha_0) \quad (3)$$

Table 1. *The values of direct, indirect bandgap and Urbach energy of the biosynthesized NiO-NPs.*

Energy (eV)		
Direct Optical bandgap	Indirect Optical bandgap	Urbach energy
3.02	3.40	2.00

Table 2. *Reports on the band gap energy values of NiO-NPs.*

S. No	Energy gap (eV)	Refs.
1	3.30	[50]
2	3.41	[46]
3	3.51	[51]
4	2.51	[52]
5	3.40	[53]
6	3.47	[41]
7	3.13	[54]
8	3.00	[55]
9	3.47	[56]
10	3.40	**Present work**

3.1.2. Fourier Transform Infrared Spectroscopy (FTIR)

Identification by FTIR analysis shows the potential presence of reducing and stabilizing biomolecules in the extract of the plant H. Hirsuta. The surface functional group of the synthesized NiO-NPs was obtained by FT-IR transmission spectra and is shown in figure 5. In general, the absorption band of interatomic vibrations, especially of metal oxides, has bands smaller than 800 cm^{-1}, the recorded peak at 432 cm^{-1} represent the appearance of Ni-O bonds [43, 46], while the double band of 1387 and 1632 cm^{-1} corresponds to the vibration mode of aromatic and carbonyl groups, respectively. The observed peak at 2942 cm^{-1} was related to the vibration of C-H bonds [47], and the broad absorption band with a peak centered at 3444 cm^{-1} is attributed to the vibration of hydroxyl group [26]. Thus, the obtained spectrum shows that the NiO-NPs synthesized in this way are a very pure phase and confirm the XRD analysis scheme.

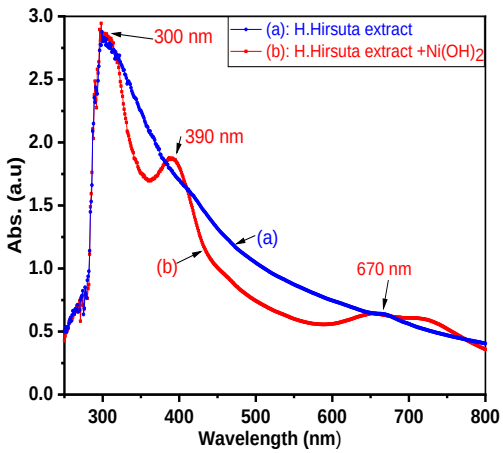

Figure 1. *UV-visible Spectrum (a) of plant Extract of H. Hirsuta, and (b) of $Ni(OH)_2$ in solution.*

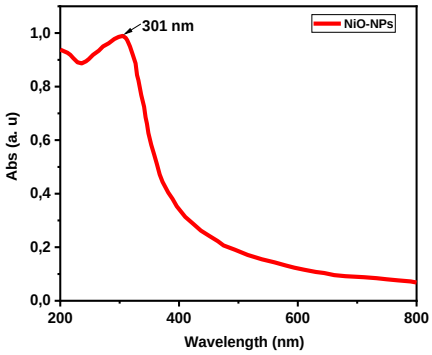

Figure 2. *UV-visible Spectrum (b) of NiO-NPs calcined at 500°C.*

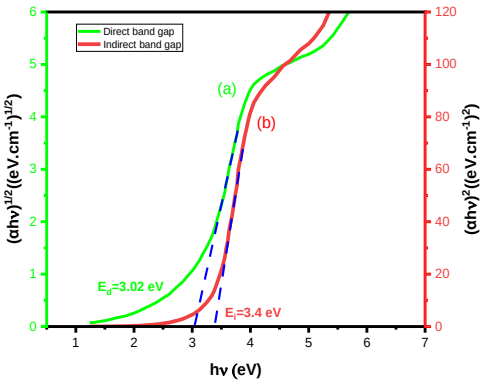

Figure 3. *Determination of the optical bandgap for (a) the direct transition and (b) the indirect transition using the Tauc method.*

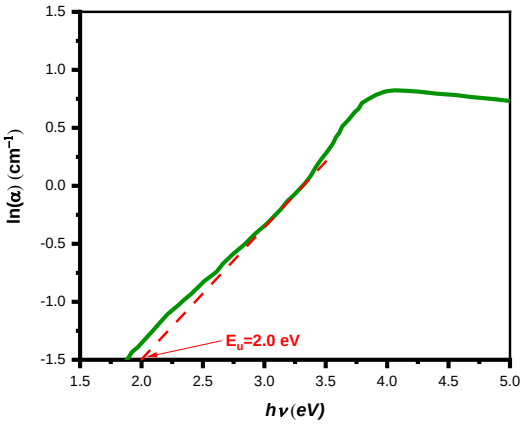

Figure 4. *Plot ln(α) versus energy: Urbach energy estimate for biosynthesized NiO-NPs.*

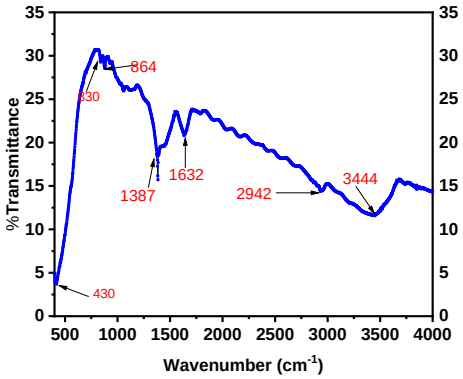

Figure 5. *FTIR spectrum of nanoparticles biosynthesized* NiO-*NPs.*

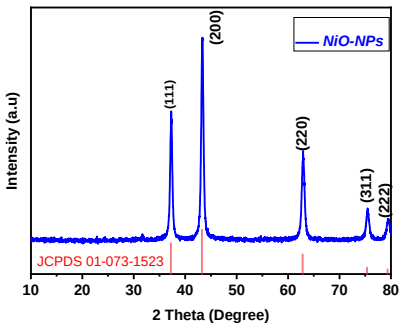

Figure 6. *XRD diagram of biosynthesized NiO-NPs.*

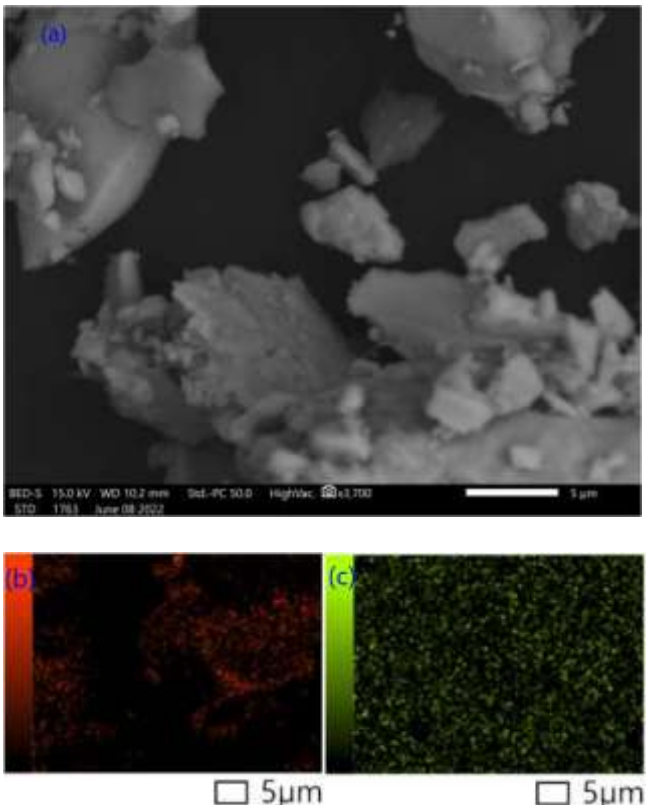

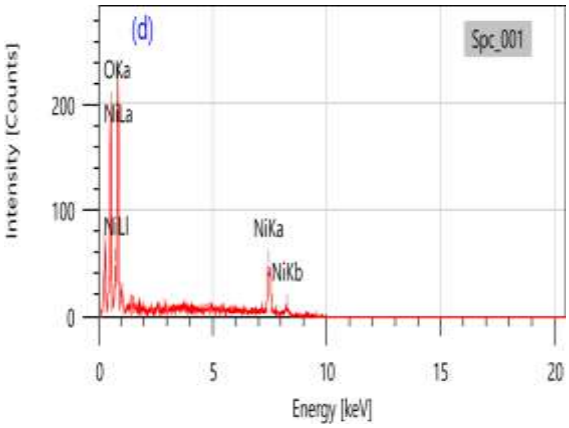

Figure 7. *(a) FESEM images of NiO-NPs biosynthesized, (b,c) corresponding EDS elemental mapping of O and Ni, (d) EDS spectrum of NiO-NPs biosynthezed.*

3.1.3. X-ray Diffraction (XRD)

X-ray diffraction is a viable tool to characterize the solid-state structure of nanomaterials. XRD analysis was used to characterize nickel oxide NPs after calcination at 500 °C. The XRD pattern of the NPs fabricated by the green route is shown in Fig. 6. The diffraction peaks observed at angles of 37.25, 43.41, 62.95, 75.43 and 79.25 were related to the (111), (200), (220), (311) and (222) crystal planes. By comparing the XRD diffractogram of the synthesized nanoparticles with the standard sample, the final diffraction pattern (JCPDS card no. 01-073-1523) [48] revealed that the synthesized NiO NPs have a cubic crystal structure (FCC) and a space group of (Fm-3m) [49]. The crystallite size of the biosynthesized NiO NPs nanoparticles was calculated using Scherrer's formula Eq. (4) considering the most intense peak at the 2θ value of 43.414°:

$$D = \frac{0.9\times\lambda}{\beta\times cos\theta} \qquad (4)$$

Where D is the crystal size (nm), β is the total width at half the diffraction peak maximum (FWHM) of the most intense diffraction peak, θ is the Bragg diffraction angle, and λ is the X-ray wavelength (for Cu-K_α, λ= 1.5406 Å). Its value was 24.3 nm, and the average crystal size is 20.82 nm, and the structural parameters are shown in table 3.

Table 3. *The structural parameters of the biosynthesized NiO-NPs.*

Peak no.	2θ (Degree)	(hkl) planes	FWHM (β)	D Crystallite size (nm)
1	37,252	111	0.12	17.8
2	43,414	200	0.096	24.3
3	62,952	220	0.264	16.4
4	75,431	311	0.12	23.7
5	79,257	222	0.336	21.9
Average crystallite size				20.82

3.1.4. Morphological Study by Scanning Electron Microscopy (FESEM/EDS)

SEM was used to study the morphology of NiO-NPs and their morphological size. The EDS of the NiO NPs is shown in Figure 7(d). It is clearly indicated that the synthesized NPs consist of Ni and O. This confirms the purity of the NiO NPs and no other impurities were detected in the sample spectrum. The weight percentage observed from the energy dispersion spectra is presented in table 4. which shows that the formed nanoparticles are rich in nickel relative to oxygen, and confirms the purity of the biosynthesized NiO-NPs. The SEM mapping images of the NiO NPs are shown in figure 7(b,c). The SEM images show an irregular spherical morphology with different particle sizes due to agglomeration (Fig. 7(a)). The surface area is high, which is beneficial for photocatalytic activity [12] [29].

Table 4. *Analysis EDS of the biosynthesized NiO-NPs.*

Element	Weight(%)
Ni	95.57
O	4.43
Total	100

3.2. Catalytic Activity for MB and Rh B Degradation

The comparative study of the efficiency of the NiO-NPs catalyst for the degradation of MB and Rh B dyes was studied under conditions optimized by S. D. KHAIRNAR and al. (for MB at pH=10 and for Rh B at pH=2) with a dye concentration of 5 mg/L and a catalyst

dose of 1 mg/L [1]. The results are shown in figure 8(a-b). MB degradation showed a steady reduction with increasing irradiation time under visible light. The decoloration of the dye solution occurred within 120 minutes of irradiation. The corresponding degradation rate of MB is 97.19%. For Rh-B, the degradation gradually increases with irradiation time and reaches equilibrium. This is due to the formation of zwitterions that occupy the active sites of the catalyst. Therefore, the degradation of Rh B does not exceed 79.42% at the same time (figure 9(a-b)). The data were used for the kinetic study of MB and Rh B dyes in the presence of NiO-NPs which shows that the degradation reactions of MB and Rh B dyes are pseudo-first-order reactions. Analysis of the kinetic data of the degradation reaction showed that the reaction kinetics is pseudo-first order. The reaction rate is determined by the following relationship: $ln(C_0/C_t) = K \times t$, where C_t and C_0 represent the concentration of the dye after and before degradation, respectively. The slope of the curve determines the value of K (min^{-1}). The linear plot of $ln(C_0/C_t)$ versus time (fig. 10(a-b)) affirms the kinetic theory, The photocatalytic activity can be compared with the value of k and the linear regression coefficient (R^2) for the solutions of MB and Rh B. The values of k, which are obtained by linear fitting of each curve, are 2.073×10^{-2} min^{-1} for MB and 1.287×10^{-2} min^{-1} for Rh-B. The photocatalytic degradation mechanism can be explained by the following equations.

$$NiO + hv \longrightarrow e^- + h^+$$

$$OH^- + h^+ \longrightarrow {}^{\cdot}OH$$

$$H_2O + h^+ \longrightarrow OH + H+$$

$$O_2 + e^- \longrightarrow {}^{\cdot}O^-$$

$$O_2^- \longrightarrow HO_2$$

$$2H_2O \longrightarrow O_2 + H_2O_2$$

$$H_2O_2 + O_2 \longrightarrow {}^{\cdot}OH + OH^- + O_2$$

$$Dye + {}^{\cdot}OH + {}^{\cdot}O_2 \longrightarrow CO_2 + H_2O + Inorg.salts.$$

The catalytic performance of NiO-NPs is related to their irregular morphology that allows the rapid movement of electrons on the catalyst surface, and their small size (average size of 20.82 nm) ensures a large specific surface area that facilitates the dyes degradation reaction by the nickel oxide nanocatalyst, which reaches the rate of 97.19% and 79.42% after an irradiation 120 min. Then, these two characteristics of biosynthesized NiO-NPs accelerate the degradation process of the BM and Rh B dyes. The photocatalytic degradation efficiencies of MB and Rh-B dyes by some metal oxide nanoparticles were compared in table 5.

Table 5. *Comparison of photocatalytic degradation efficiency of MB and Rh B dyes by some metal oxide nanoparticles.*

Photocatalysts	% Degradation MB	Rh B	Ref.
Fe_2O_3-CuO-ZnO	79		[57]
CdO-NiO-ZnO	86		[58]
CdO-ZnO		97.6	[59]
GO-Fe_3O_4-ZrO_2		98	[60]
NiO-CdO-ZnO	98	99	[61]
NiO	60		[54]
NiO	**97.**	**79.42**	**Present work**

Figure 11. describes a simple mechanism that explains the enhanced photocatalytic activity of NiO-NPs. The shape and effective surface area of the nanoparticles are two crucial parameters that can improve photocatalytic performance. A large surface area increases the photocatalytic efficiency and the absorption of reagents. Collisions between sunlight and the photocatalyst nanoparticles require less energy to excite electrons from the valence band (VB) to the conduction band (CB) in semiconductor space, producing more photons that stimulate the valence band electrons [62]. Subsequently, this electron excitation generates an equal number of holes in the valence band, and the stimulated electrons can directly or indirectly produce radical hydroxides.

Through the process of electron loss, hydroxide ions are converted into hydroxyl radicals ($OH^{\bullet}$), which are an integral part of the conversion of organic matter into minerals. This conversion is essential for the removal of MB and Rh B dyes. In addition, these organic compounds are broken down by the loss of electrons, resulting in their transformation into H_2O and CO_2, which are ultimately returned to the atmosphere [50].

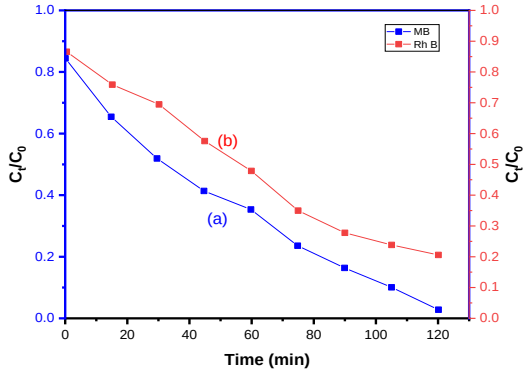

Figure 8. *Plot of (C_t/C_0) versus time for the reaction of (a) MB, and (b) Rh B with NiO-NPs.*

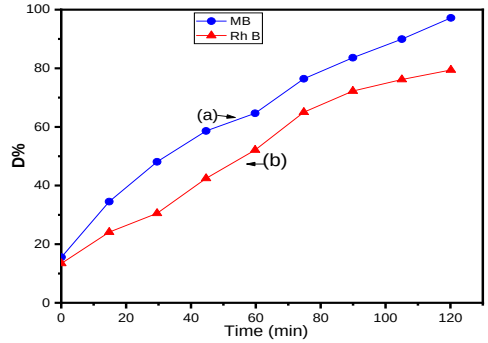

Figure 9. *Photocatalytic degradation (a) MB, conditions pH=10, dye concentration 5 mg/L and catalyst dose 1 mg/L. (b) Rh B, conditions: pH=2, dye concentration 5 mg/L and catalyst dose 1 gm/L.*

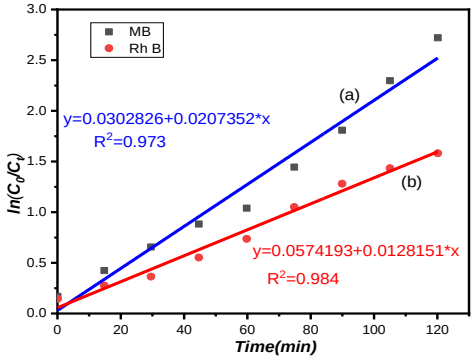

Figure 10. *Plot of $ln(C_0/C_t)$ versus time for the reaction of catalytic reduction of (a) MB, and (b) of Rh B with NiO-NPs.*

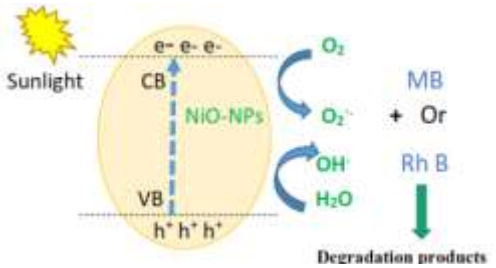

Figure 11*. Schematic plan of NiO-NPs photocatalytic mechanism.*

3.3. Catalytic Reduction of 4-NP by NiO-NPs

The catalytic reduction of 4-NP to 4-aminophenol (4-AP) was chosen to study the catalytic activity of the prepared NiO NPs. The absorption band of 4-NP appears at 317 nm, when the freshly prepared $NaBH_4$ solution is added, the light-yellow color of 4-NP changes to light yellow due to the formation of 4-nitrophenolate ions, and the absorption band moves to 400 nm. When the reduction of 4-nitrophenolate begins, the intensity of the band at 400 nm decreases with the appearance of a new band at 300 nm due to 4-AP. In addition, 4-NP is not reduced by $NaBH_4$ in the absence of catalyst. As can be seen from the UV-vis spectra (Fig.12), NiO-NPs show a reduction activity of 91.7% of 4-NP during 10 min. Since an excessive amount of $NaBH_4$ was used in these experiments, the reaction is therefore independent of the sodium borohydride concentration. The kinetic data fit according to the first-order rate equation of NiO, and straight lines are obtained by plotting $\ln(C_t/C_0)$ versus time (Fig.13) and their slope gives the value of the rate constant, which is 2.43 $\times 10^{-2}$ min^{-1}. The possible mechanism of catalytic reduction of 4-NP using $NaBH_4$ on NiO-NPs occurs in 4 steps [27]: In the first step, BH_4^- releases hydride ions into the aqueous medium, which bind to the surface of NiO. In the second step, hydrogen is covalently bound to the NiO surface. Rate-limiting

step, the adsorption of nitro groups on the surface of NiO (step 3). In addition, the adsorbed 4-NP and the bound hydrogen atoms interact strongly. The hydride ion attacks the adsorbed nitro groups, electron transfer occurs from the BH_4^- donor to the 4-NP acceptor, followed by desorption of 4-AP into the aqueous medium.

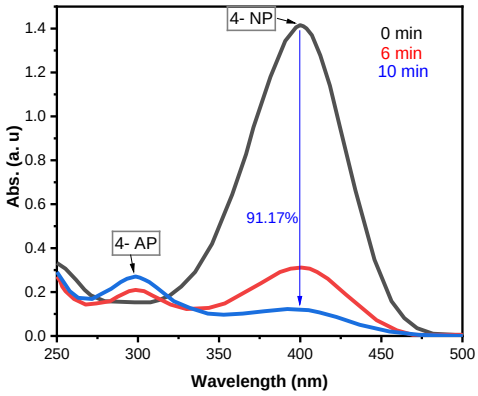

***Figure 12**. UV spectrum for the conversion of 4-NP to 4-AP using NiO-NPs.*

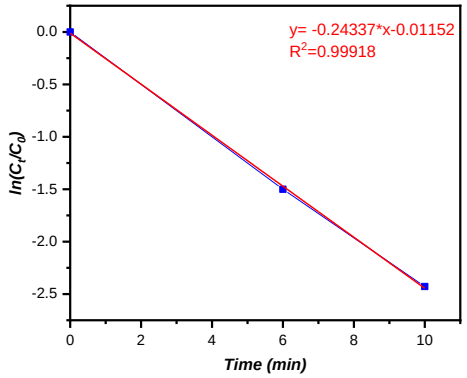

***Figure 13.** Plot of $ln(C_t/C_0)$ versus time for the reaction of catalytic reduction of 4-NP with NiO-NPs.*

4. CONCLUSION

In this study, we successfully synthesized nickel oxide nanoparticles (NiO-NPs) using a simple and environmentally friendly green synthesis method. The nanoparticles were prepared using H. Hirsuta plant extract, resulting in NiO-NPs with excellent stability and recyclability for the disposal of hazardous dyes. The synthesized NiO-NPs were characterized using a variety of analytical techniques, including UV-vis, XRD, SEM, EDS, and FTIR. Characterization revealed that the biosynthesized NiO-NPs exhibited an irregular shape, with an average crystallite size of 20.82 nm. In addition, the nanoparticles possessed direct and indirect gap energies of 3.02 and 3.42 eV, respectively, with an Urbach value measured at 2.0 eV. These results provide valuable insights into the structural and optical properties of the synthesized NiO NPs.

ACKNOWLEDGEMENT

The authors wish to thank the Centre for Research and Analysis and Characterization (CRAC) at the Faculty of Science and Technology of Settat, which provided us with the necessary analyses.

CONFLICT OF INTEREST

No potential conflict of interest was reported by the author(s).

REFERENCES

1. Khairnar, S. D., Shrivastava, V. S., "Facile synthesis of nickel oxide nanoparticles for the degradation of Methylene blue and Rhodamine B dye: a comparative study", *Journal of Taibah University for Science*, 13 (2019) 1108-1118.
2. Cai, Z., Sun, Y., Liu, W., Pan, F., Sun, P., Fu, J., "An overview of nanomaterials applied for removing dyes from wastewater", *Environmental Science and Pollution Research*, 24 (2017) 15882-15904.
3. Chaudhary, K., Aadil, M., Zulfiqar, S., Ullah, S., Haider, S., Agboola, P. O., Warsi, F. M., Shakir, I., "Graphene oxide and reduced graphene oxide supported ZnO nanochips for removal of basic dyes from the industrial effluents", *Fullerenes, Nanotubes and Carbon Nanostructures*, 29 (2021) 915-928.
4. Büyüközkan, G., Göçer, F., "Digital Supply Chain: Literature review and a proposed framework for future research", *Computers in Industry*, 97 (2018) 157-177.
5. Alimirzaeva, Z. M., Isaev, A. B., Shabanov, N. S., Magomedova, A. G., Kadiev, M. V., Kaviyarasu, K., "Photoelectrocatalytic activity PbO2 loaded highly oriented TiO2 nanotubes arrays", *Materials Today: Proceedings*, 36 (2021) 325-327.

6. Hu, W., Chu, D., Wang, L., Chen, X., Yang, H., Sun, J., "Ultrasound-assisted synthesis of hexagonal cone-like Cu2O architectures with enhanced photocatalytic activity", *Nano-Structures & Nano-Objects*, 12 (2017) 220-228.
7. Li, J., Liu, Z., Wang, D., Zhu, Z., "Visible-light responsive carbon–anatase–hematite core–shell microspheres for methylene blue photodegradation", *Materials science in semiconductor processing*, 27 (2014) 950-957.
8. Singh, J., Dutta, T., Kim, K. H., Rawat, M., Samddar, P., Kumar, P., "Green'synthesis of metals and their oxide nanoparticles: applications for environmental remediation", *Journal of nanobiotechnology*, 16 (2018) 1-24.
9. Ahmed, S. F., Mofijur, M., Rafa, N., Chowdhury, A. T., Chowdhury, S., Nahrin, M., Saiful Islam, A. B. M., Ong, H. C., "Green approaches in synthesising nanomaterials for environmental nanobioremediation: Technological advancements, applications, benefits and challenges", *Environmental Research*, 204 (2022) 111967.
10. Chavali, M. S., Nikolova, M. P., "Metal oxide nanoparticles and their applications in nanotechnology", *SN applied sciences*, 1 (2019) 1-30.
11. Kalita, C., Saikia, P., "Magnetically separable tea leaf mediated nickel oxide nanoparticles for excellent photocatalytic activity", *Journal of the Indian Chemical Society*, 98 (2021) 100213.
12. Wan, X., Yuan, M., Tie, S. L., Lan, S., "Effects of catalyst characters on the photocatalytic activity and process of NiO nanoparticles in the degradation of methylene blue", *Applied Surface Science*, 277 (2013) 40-46.
13. Thirbika, S., Karthi, H., Premila, R., Prabhu, M. R., "Investigations on biosynthesized nickel oxide nanoparticles using Cymbopogon citratus leaf extract for antibacterial activity", *Materials Today: Proceedings*, (2022).
14. Ameen, F., Srinivasan, P., Selvankumar, T., Kamala-Kannan, S., Al Nadhari, S., Almansob, A., Dawoud, T., Govarthanan, M., "Phytosynthesis of silver nanoparticles using Mangifera indica flower extract as bioreductant and their broad-spectrum antibacterial activity", *Bioorganic Chemistry*, 88 (2019) 102970.
15. Shah, A., Haq, S., Rehman, W., Waseem, M., Shoukat, S., Rehman, M. U., "Photocatalytic and antibacterial activities of paeonia emodi mediated silver oxide nanoparticles", *Materials Research Express*, 6 (2019) 045045.
16. Esmaile, F., Koohestani, H., Abdollah-Pour, H., "Characterization and antibacterial activity of silver nanoparticles green synthesized using Ziziphora clinopodioides extract", *Environmental nanotechnology, monitoring & management*, 14 (2020) 100303.
17. Das, S., Singh, V. K., Dwivedy, A. K., Chaudhari, A. K., Dubey, N. K., "Insecticidal and fungicidal efficacy of essential oils and nanoencapsulation approaches for the development of next generation ecofriendly green preservatives for management of stored food commodities: an overview", *International Journal of Pest Management*, (2021) 1-32.
18. El-Ghmari, B., Farah, H., Ech-Chahad, A., "A new approach for the green biosynthesis of Silver Oxide nanoparticles Ag2O, characterization and catalytic application", *Bulletin of Chemical Reaction Engineering & Catalysis*, 16(2021) 651-660.
19. Rashmi, B. N., Harlapur, S. F., Gurushantha, K., Ravikumar, C. R., Kumar, M. A., Santosh, M. S., Kumar, V. G. D., Kumar, A. N., Murthy, H. A., "Facile green synthesis of lanthanum oxide nanoparticles using Centella Asiatica and Tridax plants: Photocatalytic, electrochemical sensor and antimicrobial studies", *Applied Surface Science Advances*, 7 (2022) 100210.
20. Esmaile, F., Koohestani, H., Abdollah-Pour, H., "Characterization and antibacterial activity of silver nanoparticles green synthesized using Ziziphora clinopodioides extract", *Environmental nanotechnology, monitoring & management*, 14 (2020) 100303.
21. Menon, S., Rajeshkumar, S., Kumar, V., "A review on biogenic synthesis of gold nanoparticles, characterization, and its applications", *Resource-Efficient Technologies*, 3 (2017) 516-527.
22. Ovais, M., Khalil, A. T., Islam, N. U., Ahmad, I., Ayaz, M., Saravanan, M., Shinwari, K. Z., Mukherjee, S., "Role of plant phytochemicals and microbial enzymes in biosynthesis of metallic nanoparticles", *Applied microbiology and biotechnology*, 102 (2018) 6799-6814.
23. Samuel, M. S., Jose, S., Selvarajan, E., Mathimani, T., Pugazhendhi, A., "Biosynthesized silver nanoparticles using Bacillus amyloliquefaciens; Application for cytotoxicity effect on A549 cell line and photocatalytic degradation of p-nitrophenol", *Journal of Photochemistry and Photobiology B: Biology*, 202 (2020) 111642.
24. Darbandi, M., Eynollahi, M., Badri, N., Mohajer, M. F., Li, Z. A., "NiO nanoparticles with superior sonophotocatalytic performance in organic pollutant degradation", *Journal of Alloys and Compounds*, 889 (2021) 161706.

25. Akbari, A., Sabouri, Z., Hosseini, H. A., Hashemzadeh, A., Khatami, M., Darroudi, M., "Effect of nickel oxide nanoparticles as a photocatalyst in dyes degradation and evaluation of effective parameters in their removal from aqueous environments", *Inorganic Chemistry Communications*, 115 (2020) 107867.
26. Boudiaf, M., Messai, Y., Bentouhami, E., Schmutz, M., Blanck, C., Ruhlmann, L., Bezzi, H., Tairi, A., Mekki, D. E., "Green synthesis of NiO nanoparticles using Nigella sativa extract and their enhanced electro-catalytic activity for the 4-nitrophenol degradation", *Journal of Physics and Chemistry of Solids*, 153 (2021) 110020.
27. Bhatia, P., Nath, M., "Green synthesis of p-NiO/n-ZnO nanocomposites: Excellent adsorbent for removal of congo red and efficient catalyst for reduction of 4-nitrophenol present in wastewater", *Journal of Water Process Engineering*, 33 (2020) 101017.
28. Tiwari, B., Choudhary, R. N. P., "Effect of Mn-substitution on structural and dielectric properties of Pb (Zr0. 65− xMnxTi0. 35) O3 ceramics", *Solid State Sciences*, 11 (2009) 219-223.
29. Adinaveen, T., Karnan, T., Selvakumar, S. A. S., "Photocatalytic and optical properties of NiO added Nephelium lappaceum L. peel extract: An attempt to convert waste to a valuable product", *Heliyon*, 5 (2019) e01751.
30. Farhadi, S., Kazem, M., Siadatnasab, F., "NiO nanoparticles prepared via thermal decomposition of the bis (dimethylglyoximato) nickel (II) complex: A novel reusable heterogeneous catalyst for fast and efficient microwave-assisted reduction of nitroarenes with ethanol", *Polyhedron*, 30 (2011) 606-613.
31. Ramasami, A. K., Reddy, M. V., Balakrishna, G. R., "Combustion synthesis and characterization of NiO nanoparticles", *Materials Science in Semiconductor Processing*, 40 (2015) 194-202.
32. Zorkipli, N. N. M., Kaus, N. H. M., Mohamad, A. A., "Synthesis of NiO nanoparticles through sol-gel method", *Procedia chemistry*, 19 (2016) 626-631.
33. Ghazal, S., Akbari, A., Hosseini, H. A., Sabouri, Z., Forouzanfar, F., Khatami, M., Darroudi, M., "Sol-gel biosynthesis of nickel oxide nanoparticles using Cydonia oblonga extract and evaluation of their cytotoxicity and photocatalytic activities", *Journal of Molecular Structure*, 1217 (2020) 128378.
34. Rahman, M. A., Radhakrishnan, R., Gopalakrishnan, R., "Structural, optical, magnetic and antibacterial properties of Nd doped NiO nanoparticles prepared by co-precipitation method", *Journal of Alloys and Compounds*, 742 (2018) 421-429.
35. Wang, W. N., Itoh, Y., Lenggoro, I. W., Okuyama, K., "Nickel and nickel oxide nanoparticles prepared from nickel nitrate hexahydrate by a low pressure spray pyrolysis", *Materials Science and Engineering: B*, 111 (2004) 69-76.
36. Wei, Z., Qiao, H., Yang, H., Zhang, C., Yan, X., "Characterization of NiO nanoparticles by anodic arc plasma method", *Journal of alloys and compounds*, 479 (2009) 855-858.
37. Gebretinsae, H. G., Tsegay, M. G., Nuru, Z. Y., "Biosynthesis of nickel oxide (NiO) nanoparticles from cactus plant extract", *Materials Today: Proceedings*, 36 (2021) 566-570.
38. Bahammou, Y., Moussaoui, H., Lamsayeh, H., Tagnamas, Z., Kouhila, M., Ouaabou, R., Lamharrar, A., Idlimam, A., "Water sorption isotherms and drying characteristics of rupturewort (Herniaria hirsuta) during a convective solar drying for a better conservation", *Solar Energy*, 201 (2020) 916-926.
39. Van Dooren, I., Faouzi, M. E. A., Foubert, K., Theunis, M., Pieters, L., Cherrah, Y., Apers, S., "Cholesterol lowering effect in the gall bladder of dogs by a standardized infusion of Herniaria hirsuta L.", *Journal of ethnopharmacology*, 169 (2015) 69-75.
40. Qi, Y., Qi, H., Li, J., Lu, C., "Synthesis, microstructures and UV–vis absorption properties of β-Ni (OH) 2 nanoplates and NiO nanostructures", *Journal of crystal growth*, 310 (2008) 4221-4225.
41. Sabouri, Z., Akbari, A., Hosseini, H. A., Khatami, M., Darroudi, M., "Green-based bio-synthesis of nickel oxide nanoparticles in Arabic gum and examination of their cytotoxicity, photocatalytic and antibacterial effects", *Green Chemistry Letters and Reviews*, 14 (2021) 404-414.
42. Fall, A., Sackey, J., Mayedwa, N., Ngom, B. D., "Investigation of structural and optical properties of CdO nanoparticles via peel of Citrus x sinensis", *Materials Today: Proceedings*, 36 (2021) 298-302.
43. Ramesh, R., Yamini, V., Sundaram, S. J., Khan, F. L. A., Kaviyarasu, K., "Investigation of structural and optical properties of NiO nanoparticles mediated by Plectranthus amboinicus leaf extract", *Materials Today: Proceedings*, 36 (2021) 268-272.
44. Yousaf, S., Zulfiqar, S., Shahi, M. N., Warsi, M. F., Al-Khalli, N. F., Aboud, M. F. A., Shakir, I., "Tuning the structural, optical and electrical properties of NiO nanoparticles prepared by wet chemical route", *Ceramics International*, 46 (2020) 3750-3758.
45. Amor, M. B., Boukhachem, A., Boubaker, K., Amlouk, M., "Structural, optical and electrical studies on Mg-doped NiO thin films for sensitivity applications", *Materials science in semiconductor processing*, 27 (2014) 994-1006.
46. Kannan, K., Radhika, D., Nikolova, M. P., Sadasivuni, K. K., Mahdizadeh, H., Verma, U., "Structural studies of bio-mediated NiO nanoparticles for photocatalytic and antibacterial activities", *Inorganic Chemistry Communications*, 113 (2020) 107755.

47. Miri, A., Mahabbati, F., Najafidoust, A., Miri, M. J., Sarani, M., "Nickel oxide nanoparticles: biosynthesized, characterization and photocatalytic application in degradation of methylene blue dye", *Inorganic and Nano-Metal Chemistry*, 52 (2022) 122-131.
48. Bhatia, P., Nath, M., "Nanocomposites of ternary mixed metal oxides (Ag2O/NiO/ZnO) used for the efficient removal of organic pollutants", *Journal of Water Process Engineering*, 49 (2022) 102961.
49. Aravind, M. R., Kalaiselvi, C., Revathi, B., Grace, A. N., Pitchaimuthu, S., Suresh, S., Sindhu, M., Chandar, N. K., "Influence of various concentrations of cetyltrimethylammonium bromide on the properties of nickel oxide nanoparticles for supercapacitor application", *Nano*, 16 (2021) 2150138.
50. Sabouri, Z., Akbari, A., Hosseini, H. A., Khatami, M., Darroudi, M., "Egg white-mediated green synthesis of NiO nanoparticles and study of their cytotoxicity and photocatalytic activity", *Polyhedron*, 178 (2020) 114351.
51. Karthik, K., Shashank, M., Revathi, V., Tatarchuk, T., "Facile microwave-assisted green synthesis of NiO nanoparticles from Andrographis paniculata leaf extract and evaluation of their photocatalytic and anticancer activities", *Molecular Crystals and Liquid Crystals*, 673 (2018) 70-80.
52. Sabouri, Z., Akbari, A., Hosseini, H. A., Hashemzadeh, A., Darroudi, M., "Bio-based synthesized NiO nanoparticles and evaluation of their cellular toxicity and wastewater treatment effects", *Journal of Molecular Structure*, 1191 (2019) 101-109.
53. Sabouri, Z., Akbari, A., Hosseini, H. A., Hashemzadeh, A., Darroudi, M., "Eco-Friendly Biosynthesis of Nickel Oxide Nanoparticles Mediated by Okra Plant Extract and Investigation of Their Photocatalytic, Magnetic, Cytotoxicity, Antibacterial Properties", *J Clust Sci.*, 30 (2019) 1425-1434.
54. Sabouri, Z., Akbari, A., Hosseini, H. A., Khatami, M., Darroudi, M., "Tragacanth-mediate synthesis of NiO nanosheets for cytotoxicity and photocatalytic degradation of organic dyes", *Bioprocess Biosyst Eng*, 43 (2020) 1209-1218.
55. Sabouri, Z., Sabouri, M., Amiri, M. S., Khatami, M., Darroudi, M., "Plant-based synthesis of cerium oxide nanoparticles using Rheum turkestanicum extract and evaluation of their cytotoxicity and photocatalytic properties", *Materials Technology*, 37 (2022) 555-568.
56. Sabouri, Z., Rangrazi, A., Amiri, M. S., Khatami, M., Darroudi, M., "Green synthesis of nickel oxide nanoparticles using Salvia hispanica L. (chia) seeds extract and studies of their photocatalytic activity and cytotoxicity effects", *Bioprocess Biosyst Eng*, 44 (2021) 2407-2415.
57. Tju, H., Taufik, A., Saleh, R., "Enhanced UV Photocatalytic Performance of Magnetic Fe3O4/CuO/ZnO/NGP Nanocomposites", *J. Phys.: Conf. Ser*., 710 (2016) 012005.
58. Karthik, K., Dhanuskodi, S., Gobinath, C., Prabukumar, S., Sivaramakrishnan, S., "Multifunctional properties of microwave assisted CdO–NiO–ZnO mixed metal oxide nanocomposite: enhanced photocatalytic and antibacterial activities", *J Mater Sci: Mater Electron*, 29 (2018) 5459-5471.
59. Linda, T., Muthupoongodi, S., Shajan, X. S., Balakumar, S.,"Fabrication and characterization of chitosan templated CdO/NiO nano composite for dye degradation", *Optik*, 127 (2016) 8287-8293.
60. El-Shafai, N. M., El-Khouly, M. E., El-Kemary, M., Ramadan, M. S., Masoud, M. S., "Graphene oxide–metal oxide nanocomposites: fabrication, characterization and removal of cationic rhodamine B dye", *RSC Adv.*, 8 (2018) 13323-13332.
61. Munawar, T., Iqbal, F., Yasmeen, S., Mahmood, K. Hussain, A., "Multi metal oxide NiO-CdO-ZnO nanocomposite–synthesis, structural, optical, electrical properties and enhanced sunlight driven photocatalytic activity", *Ceramics International*, 46 (2020) 2421-2437.
62. Aboelfetoh, E. F., Aboubaraka, A. E., Ebeid, E. Z. M., "Synergistic Effect of Iron and Copper Oxides in the Removal of Organic Dyes Through Thermal Induced Catalytic Degradation Process", *Journal of Cluster Science*, (2023) 1-15.